ROD-SAN: Energy-Efficient and High-Response Wireless Sensor and Actuator Networks Employing Wake-Up Receiver*

Hiroyuki YOMO[†a)], *Member*, Takahiro KAWAMOTO[†], Kenichi ABE[††], *Nonmembers*, Yuichiro EZURE[††],
Tetsuya ITO[††], Akio HASEGAWA[†††], *and* Takeshi IKENAGA[††††], *Members*

SUMMARY Wireless sensor and actuator networks (WSANs) are required to achieve both energy–efficiency and low–latency in order to prolong the network lifetime while being able to quickly respond to actuation commands transmitted based on the real–time sensing data. These two requirements are in general in a relationship of trade–off when each node operates with well–known duty–cycling modes: nodes need to make their radio interfaces (IFs) frequently active in order to promptly detect the communication requests from the other nodes. One approach to break this inherent trade–off, which has been actively studied in recent literature of wireless sensor networks (WSNs), is the introduction of *wake–up receiver* that is installed into each node and used only for detecting the communication requests. The main radio IF in each node is woken up only when needed, i.e., in an on–demand manner, through a wake–up message received by the wake–up receiver. In this paper, we introduce radio–on–demand sensor and actuator networks (ROD–SAN) where the concept of wake–up receiver is applied to realize on–demand WSANs. We first evaluate data collection rate, packet delivery latency, and energy–efficiency of ROD–SAN and duty–cycling modes defined in IEEE 802.15.4e by computer simulations. Then, we present our test–bed implementation of ROD–SAN including all protocols from the lowest layer of wake–up signaling to the application layer offering the functionalities of information monitoring and networked control. Finally, we show experimental results obtained through our field trial in which 20 nodes are deployed in an outdoor area with the scale of $450\,\text{m} \times 200\,\text{m}$. The numerical results obtained by computer simulations and experiments confirm the effectiveness of ROD–SAN to realize energy–efficient and high–response WSANs.
key words: wireless sensor and actuator networks, wake–up receiver, duty–cycling, experimental prototype and implementation

1. Introduction

Wireless sensor and actuator networks (WSANs) [1] play an important role to realize applications involving network–based monitoring and control in different fields such as industrial monitoring and control [2], building automation [3], and smart–grid [4]. WSANs share many key requirements with wireless sensor networks (WSNs) such as *energy–*

efficiency that comes from limitations on the lifetime of batteries. Furthermore, the inclusion of actuators into each node brings another key requirement in WSANs, i.e., *low–latency* that is necessary to realize quick reactions to control commands transmitted based on the real–time monitoring information.

The most common approach to realizing energy–efficient operations in WSN is *duty–cycling* [5] in which each node employs periodical activations and sleeping (i.e., switch–off) of radio interface (IF). For instance, IEEE 802.15.4e, that is the amendment of IEEE 802.15.4 to enhance energy–efficiency of WSN, defines several duty–cycling modes such as coordinated sampled listening (CSL) and receiver initiated transmission (RIT) [6]. While the duty–cycling can effectively reduce energy consumed for idle listening, it has inherent trade–off with latency: when nodes employ lower duty–cycle in order to save more energy, it has to sacrifice the latency since each transmitter needs to wait for longer period before the corresponding receiver transits to an active state. This makes it difficult for the duty–cycling to simultaneously offer key requirements on WSANs, i.e., energy–efficiency and low–latency.

One solution to overcome the above inherent trade–off of duty–cycling is the introduction of secondary radio called *wake–up receiver* into each node [7]. During idle period, each node switches its main radio IF off, and keeps only the wake–up receiver to be active. When a node transmits data, it first transmits a wake–up signal toward the destination node. If the wake–up receiver at the destination node detects the wake–up signal correctly, it activates the radio IF, followed by the data exchange through the main radio. Thanks to this *on–demand* operation, the latency is minimized while the energy–efficiency is also guaranteed as long as the energy consumption of wake–up receiver is much smaller than that of main radio. Considering that the low–latency is one of key requirements in WSANs, the application of wake–up receiver to WSANs is a reasonable approach. Therefore, in this paper, we introduce radio–on–demand sensor and actuator networks (ROD–SAN) that applies wake–up receiver to WSAN nodes [8], [9]. ROD–SAN employs IEEE 802.15.4g operating over 920 MHz as a radio technology, which makes it possible to be applied to a large–scale monitoring and control such as smart metering. Furthermore, ROD–SAN employs a wake–up signaling that can reuse IEEE 802.15.4g signal as a wake–up signal. In this paper, we present extensive evaluations of ROD–SAN based on computer simula-

tions and large–scale experiments in order to investigate its effectiveness to realize energy–efficient and high–response WSANs. The main contribution of this paper is threefold:

- We evaluate data collection rate, packet delivery latency, and energy–efficiency of ROD–SAN and two duty–cycling modes defined in IEEE 802.15.4e, i.e., CSL and RIT, by computer simulations. The evaluations reflect the overhead resulting from wake–up signaling in ROD–SAN, CSL, and RIT, and its impact on medium access control (MAC) operations in a large–scale multi–hop network. The obtained numerical results provide us with insights on the superiority of ROD–SAN to duty–cycling modes.

- We design and implement ROD–SAN including all protocols required to realize on–demand WSANs, from the lowest layer of wake–up signaling to the application layer offering the functionalities of information monitoring and networked control. We integrate the wake–up receiver with radio interface of IEEE 802.15.4g/802.15.4 and the other higher–layer protocols such as networking and application layers.

- We present experimental results obtained through our field trial in which 20 ROD–SAN nodes are deployed in an outdoor area with the scale of 450m × 200m. The results show performance of ROD–SAN when each node is engaged not only in its own data transmissions but also in networking tasks such as data forwarding and route maintenance.

The rest of the paper is organized as follows. Section 2 describes the system configuration of ROD–SAN. In Sect. 3, we present simulation results that clarify the superiority of ROD–SAN to duty–cycling modes. Section 4 shows our test–bed implementations of ROD–SAN and experimental results obtained by our field trial. Finally, Sect. 5 concludes the paper.

2. ROD–SAN: System Configuration

ROD–SAN is a wireless sensor and actuator network where each node is equipped with a wake–up receiver and on–demand multi–hop data transmissions are employed for conveying sensing and command data.

The overall configuration of ROD–SAN node and procedure of data transmission over one–hop link are depicted in Fig. 1. A typical ROD–SAN node consists of micro controller unit (MCU), sensor, actuator, battery, main radio IF and wake–up receiver. Each ROD–SAN node is not necessarily equipped with both sensor and actuator, but here, we show an example of node with both of them installed. As a main radio, we use IEEE 802.15.4g that operates over 920 MHz frequency band [10]. The wake–up receiver is dedicated to receiving a wake–up signal transmitted by a node with communication requests. When data to be transmitted is generated at one node, it first transmits a wake–up signal to the other destination node. The main radio IF is used to transmit a wake–up signal. If this signal is cor-
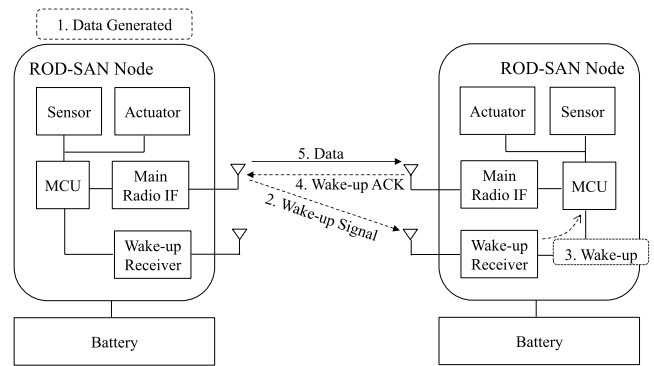

Fig. 1 The configuration of ROD–SAN node and procedure of data transmission.

rectly detected at the wake–up receiver of destination node, it wakes MCU and its main radio IF up. Then, after completing the wake-up process of main radio IF (i.e., after the sleep/active switching time), a wake–up ACK is immediately transmitted from the destination to confirm the successful wake–up, and finally data is exchanged through main radio IFs. The size of wake–up ACK is assumed to be 28 bytes that is same as ACK for data frame. If the sender does not receive the wake–up ACK before timeout, which is set to a total duration of sleep/wake-up switching time and ACK duration, it proceeds with the retransmission of wake–up signal. The maximum number of retransmissions is set to be 3. After completing the data transmission, all components but wake–up receiver can be switched off, which significantly reduces the energy consumed for idle listening of main radio.

There can be range–based and identity–based mechanisms for wake–up radio [7]. With the range–based wake–up, the wake–up receiver detecting signal level larger than a threshold wakes its radio IF up. On the other hand, a wake–up ID is embedded into wake–up signal with the identity–based wake–up, which enables only nodes specified by IDs to wake–up. The identity–based wake–up is preferred to reduce the number of unnecessary wake–ups, i.e., to avoid the events where non–destined nodes are woken up by a wake–up signal. This requires the signaling, i.e., transfer of information on wake–up ID, between the 802.15.4g–based radio at the sender side and wake–up receiver at the destination node. In order to realize this wake–up signaling, ROD–SAN exploits the length of 802.15.4g frame (that is, the length of energy burst) to convey the information on wake–up ID. The wake–up ID is expressed as different frame length, and the wake–up receiver is configured so that it only has the capability to detect the frame length without implementing any expensive operations to demodulate/decode payload/header of each frame. The block diagram of wake–up receiver is shown in Fig. 2. The received signal is first amplified with low noise amplifier (LNA) followed by the extraction of signals over 920 MHz band with a band pass filter (BPF). The output of envelope detector is smoothed with low–pass–filter (LPF) and on–off–keying (OOK) detection is applied
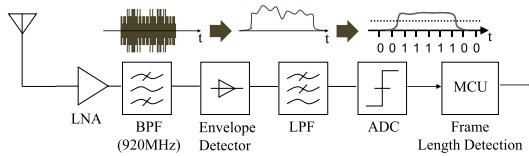
Fig. 2 The configuration of wake–up receiver in ROD–SAN.

Fig. 3 Basic operations of different schemes: (a) IEEE 802.15.4, (b) CSL, (c) RIT, and (d) ROD-SAN.

to detect the signal with its level larger than a threshold. By counting the continuous number of "1"s, MCU calculates the length of observed frame. This type of wake–up receiver has been implemented and evaluated in literature, which shows that their power consumption can be less than a few milliwatts [11].

The idea to utilize the length of frame to convey information toward a simple receiver has been applied in several different scenarios [12]–[14]. This approach does not require a dedicated transmitter of wake–up signal to be installed into each node, which brings a benefit to reduce the cost and complexity of each ROD–SAN node.

3. ROD–SAN: Performance Comparison with Duty-Cycling

As described in Sect. 2, ROD–SAN requires each node to transmit wake–up signal before each data transmission. This results in the overhead in terms of energy consumption and latency of each transmitting node, and also increases the channel occupation period. Furthermore, the wake–up receiver installed into each node needs to be always active in order to detect communication requests, which results in the additional overhead of consumed energy. Therefore, in order to investigate the superiority of ROD–SAN to duty–cycling modes, we need to evaluate their network–level performance considering MAC operations and power consumed at each operation. In this section, we compare performance of ROD–SAN and duty–cycling modes defined in IEEE 802.15.4e by computer simulation.

3.1 Duty–Cycling Modes Defined in IEEE 802.15.4e

As reference schemes for comparison, we focus on two standard duty–cycling modes defined in IEEE 802.15.4e, i.e., CSL and RIT, and standard IEEE 802.15.4 without any enhancement to improve energy–efficiency. CSL is a duty–cycling mode categorized into a transmitter–initiated protocol where a transmitter side initiates the trigger of synchronization of active states while RIT is a receiver–initiated protocol where a receiver side initiates its trigger.

Figure 3(a)–(c) show basic operations of reference schemes[†]. As shown in Fig. 3(a), nodes operating with IEEE 802.15.4 are always in active states, and transmit data following carrier sense multiple access with collision avoid-

---

[†]For simplicity of presentation, ACK transmission and switching periods between active/sleep states of each node are omitted in Fig. 3, but they are included in the implementation of all protocols in simulations.
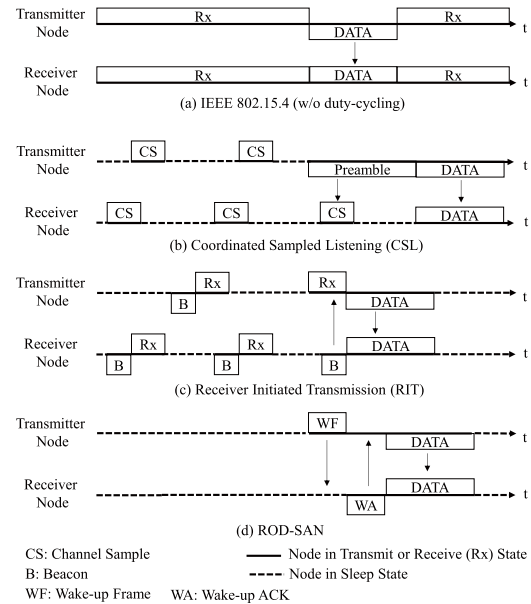
ance (CSMA/CA) defined in [15]. IEEE 802.15.4 is expected to achieve the best performance except for energy–efficiency since it can initiate data transmissions without any overhead for wake–up signaling, and used as a benchmark for the other low–power protocols. With CSL, each node periodically transits active and sleep states as shown in Fig. 3(b). Every time a node transits to active state, it checks whether there is any other node that attempts to transmit data to it with an operation called channel sample (CS). A node with communication requests first transmits a preamble whose length exceeds the period of duty–cycling, which ensures that the target node detects it with the operation of CS. The preamble includes the information on the starting time of data transmission, therefore, the receiver can transit to sleep state until the start of actual data transmission. These mechanisms enable the transmitter and receiver to synchronize their active states during which data is transmitted based on CSMA/CA. With RIT shown in Fig. 3(c), each node also periodically transits active and sleep states, but broadcasts beacon (B) after switching to active state. The beacon plays a role to announce that the corresponding node is currently active and able to receive data if there is any transmitter within its vicinity. After transmitting a beacon, each node transits to Rx state to check whether there is any transmission destined to itself. A node with communication requests waits until it receives a beacon from its destination node. Once the transmitter detects the beacon transmitted by the destination, it transmits data with CSMA/CA operations. Note that preambles and beacons are also transmitted based on CSMA in CSL and RIT, respectively. We also show the basic operation of ROD–SAN in Fig. 3(d), which was described in Sect. 2. Note that the wake–up receiver is always active in ROD–SAN though it is not shown in Fig. 3.

Table 1 Simulation parameters.

|		
Common for all schemes	Simulation Duration	1200 s
	Bit Rate	100 kbps
	Payload Length (Sensing Data)	222 bytes
	ACK Length	28 bytes
	Max. Num. of Back-offs	10
	Max. Num. of Retransmissions	3
	Power Consumption in Tx state	52.2 mW
	Power Consumption in Rx state	59.1 mW
	Power Consumption in Sleep state	0.6 mW
	Sleep/Active Switching Time [17]	2.4 ms
	CCA (Clear Channel Assessment) duration	160 μs
	SIFS	26 μs
CSL	CS duration	20 ms
RIT	Beacon Duration	5.12 ms
	Rx duration after beacon	15 ms
ROD-SAN	Power Consumption of wake-up receiver	1 mW
	Wake-up ACK Length	28 bytes
	Minimum Length of Wake-up Frame	10.8 ms
	Length Step of Wake-up Frame	160 μs
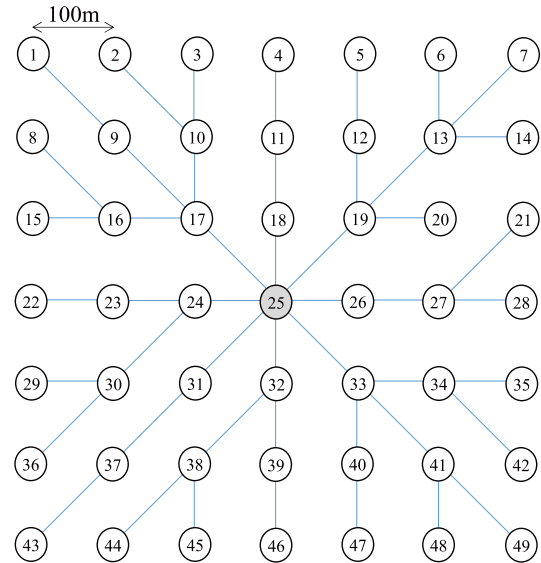
Fig. 4 Node deployment and tree routing topology constructed by RPL.

3.2 Simulation Model

In our simulation, we deploy 49 nodes with a grid topology (grid distance of 100 m) as shown in Fig. 4. We assume that the communication range (range within which all data and control frames including preamble, beacon, and wake–up frames can be successfully transmitted) is 150 m[†], and it is same as the carrier sensing range. Data and control frames can be lost only due to collisions and time–out that occurs when the number of back–offs exceeds the permitted value defined in IEEE 802.15.4. Node 25 in Fig. 4 is assumed to be a sink node where all sensing data should be collected. Since there are many nodes that have no direct link to the sink node, we employ multi–hop data transmissions. We ran RPL [16] in order to construct a tree routing topology that is shown with lines in Fig. 4. We obtained a topology with 3–hop transmissions at maximum. The other parameters employed in computer simulations are shown in Table 1. The power consumptions of Tx/Rx/sleep states are taken from [17]. For simplicity of simulation, we use the same value for sleep/active switching time for all schemes. The power consumption of wake–up receiver is assumed to be 1 mW based on the preliminary measurement of our prototype of wake–up receiver that will be presented in Sect. 4[††]. The minimum length of wake–up frame in ROD–SAN is assumed to be 10.8 ms, and we allocate different frame length corresponding to wake–up ID to different nodes with the increasing order of node number with the step length of 160 μs.

Fig. 5 Data collection rate of different schemes for different number of hops (generation period of sensing data = 60 s).

Fig. 6 Data collection rate of different schemes for different number of hops (generation period of sensing data = 5 s).

3.3 Simulation Results

Figures 5 and 6 show data collection rate (the ratio of number of sensing data correctly received at the sink node to the number of transmitted sensing data) of different schemes for

---

[†]The assumption on wake–up range is justified with our preliminary experiments presented in [9], where we confirmed that wake-up frames are accurately detected within the range of 150 m. The assumption can be also justified with the results of our field trial presented in Sect. 4.4.1, where links with their distance ranging from around 50 m to 200 m are created with ROD–SAN.

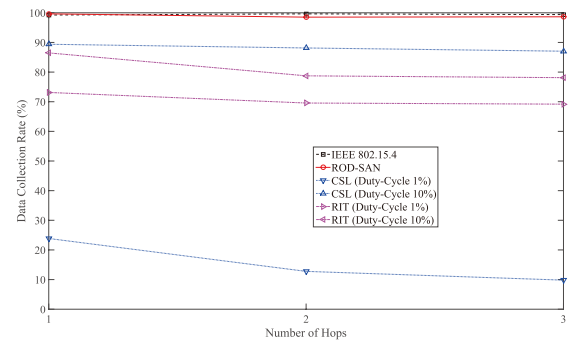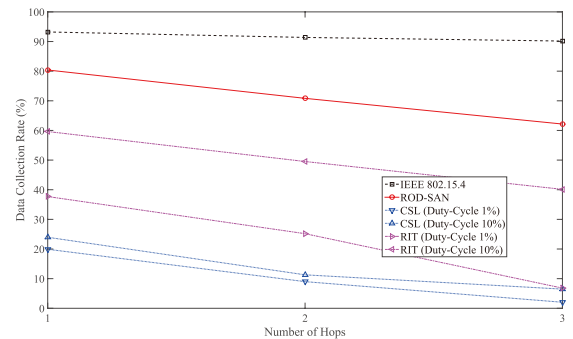[††]The power consumption of wake–up receiver can be further reduced by optimizing its circuit configuration.

Fig. 7 Data delivery latency of different schemes for different number of hops (generation period of sensing data = 60 s).

Fig. 9 Energy consumption of Node 1, 41, 17 for different schemes (generation period of sensing data = 60 s).
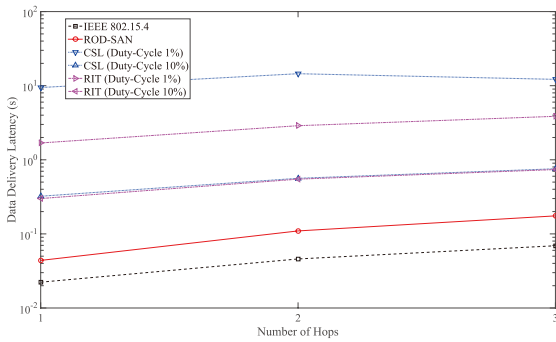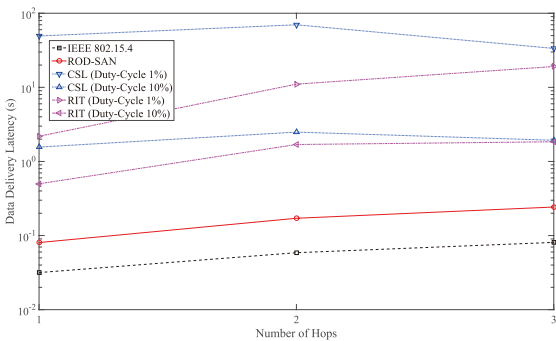

Fig. 8 Data delivery latency of different schemes for different number of hops (generation period of sensing data = 5 s).

Fig. 10 Energy consumption of Node 1, 41, 17 for different schemes (generation period of sensing data = 5 s).

nodes with different numbers of hops toward the sink node when the generation periods of sensing data are set to 60s and 5s, respectively. The results for each number of hops are obtained by averaging the data collection rates of all nodes whose number of hops toward the sink node is the same in Fig. 4. From these figures, we can first see that the data collection rate is degraded as the required number hops is increased. When the generation period of sensing data is 60s, the performance of RIT is worse than CSL with duty–cycling of 10% since the channel is relatively congested for RIT due to the requirement to periodically transmit beacons. Furthermore, the performance of CSL is severely degraded by reducing its duty–cycle to 1%. This is because much longer preamble is needed when the duty–cycle is lowered in CSL, which significantly increases the channel occupation period, resulting in more severe congestion. When the generation period of sensing data is 5s, the frequent transmissions of preambles in CSL become more severe problem than transmissions of beacons in RIT, and the performance of RIT is always better than that of CSL. Note that the performance of ROD–SAN is always better than duty–cycling modes with different duty–cycles for both generation periods of sensing data. This clearly shows the superiority of ROD–SAN to duty–cycling modes in terms of reliability to deliver sensing data.

Figures 7 and 8 show data delivery latency (the time between the generation of sensing data at each node and its

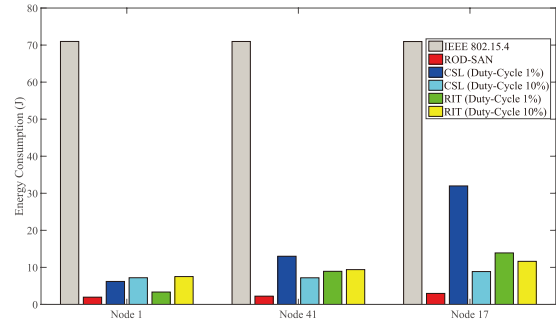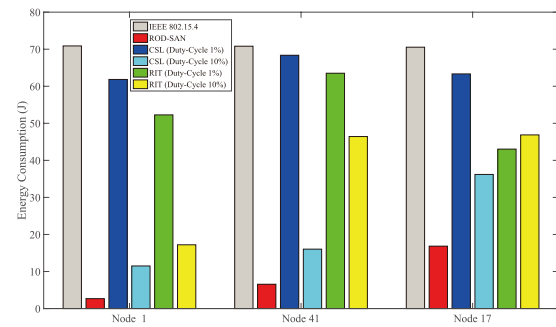correct reception at the sink node) of different schemes for nodes with different numbers of hops toward the sink node when the generation periods of sensing data are set to 60 s and 5 s, respectively. The results for each number of hops are obtained by averaging the data delivery latency of all nodes whose number of hops toward the sink node is the same in Fig. 4. In these figures, we can find the same tendency as the results on data collection rate. Furthermore, we can confirm that, while the latency is significantly increased with the reduction of duty–cycle for CSL and RIT, ROD–SAN achieves the smaller latency that is close to the value of IEEE 802.15.4.

Figures 9 and 10 show energy consumption of different schemes for some selected nodes (node 1, 17, 41) when the generation periods of sensing data are set to 60s and 5s, respectively. These nodes are located at different positions and have different number of hops toward the sink node. Let us first focus on Fig. 9 where the generation period of sensing data is 60s. From this figure, we can first see that node 17 (node 1) consumes the largest (smallest) amount of energy. Node 1 has 3 hops to reach the sink node, but it does not have to forward any data of the other nodes, which results in the smallest energy consumption. On the other hand, node 17, which is a 1-hop neighbor of the sink node, accommodates many nodes below itself within the tree topology, and needs to forward many data. This causes node 17 to consume the largest amount of energy. Node 41 has 2 hops to

deliver data to the sink node, and its energy consumption lies in the middle of the other two nodes. Next, interestingly, Fig. 9 shows that the energy consumption of CSL is increased as its duty–cycle is decreased from 10% to 1% for node 17 and node 41. This is because, in CSL, each transmitter needs to transmit longer preamble with lower duty–cycle, and the duration for each node to be in Tx state is increased as the duty–cycle is decreased. Thus, the energy consumption of CSL is dominated by the energy consumed for transmissions of preambles. Finally, we can clearly see that ROD–SAN consumes the least amount of energy out of all schemes for any node, and its reduction rate is significant. Looking at the results shown in Fig. 10 where the generation period of sensing data is decreased, it is clear that the amount of consumed energy is increased for all nodes and schemes due to more frequent transmissions of sensing data. We can notice that, for node 1 and node 41, RIT experiences larger energy consumption for lower duty–cycle. Node 1 and node 41 attempt to transmit data to their parents inside the constructed tree topology, i.e., node 9 for node 1, and node 33 for node 41. However, due to frequent transmissions and forwarding of sensing data, node 9 and node 33 are often busy to transmit their own data. This prevents these nodes from sending beacons, which makes node 1 and mode 41 wait for a longer period in Tx state before data transmission, especially when the duty–cycle is lower. This is the reason why the energy consumptions of node 1 and node 41 have much higher values for lower duty–cycle. From Fig. 10, we can clearly see that ROD–SAN consumes the least amount of energy even when the generation period of sensing data is decreased, i.e., when the network is more congested.

In order to investigate the energy consumed for idle operations of different schemes, we plot the energy consumption when the sensing data is rarely transmitted, i.e., when the generation period of sensing data is set to be 600 s in Fig. 11. By comparing Fig. 11 with Figs. 9 and 10, we can see that the energy consumption of duty–cycling modes, especially modes with lower duty–cycle, is significantly reduced as the generation period of sensing data increases. ROD–SAN requires the wake–up receiver to be always active, and its energy consumption converges to that of wake–up receiver. Since the converged value is slightly larger than the energy consumption required for duty–cycling modes with lower duty–cycle, the energy consumption of ROD–SAN is slightly larger than that of duty–cycling modes for node 1 and node 41 that have extremely low traffic load as shown in Fig. 11. However, even in this extreme case with very large period of sensing data, ROD–SAN shows superiority in terms of energy consumption for node 17 that is a 1-hop neighbor of the sink node and has relatively higher traffic load than the other nodes due to the necessity of data forwarding.

Due to lack of space, we do not show results here, but we confirmed that ROD–SAN has the smallest amount of energy averaged over all nodes in the network. We also checked the energy consumption of a node that consumes
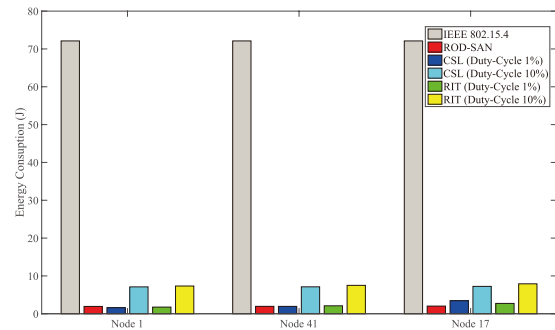

Fig. 11   Energy consumption of Node 1, 41, 17 for different schemes (generation period of sensing data = 600 s).

the largest amount of energy in the network, and found that ROD–SAN can also reduce this maximum amount of energy consumption significantly.

From all the above results, we can conclude that ROD–SAN can achieve higher reliability, energy–efficiency and lower latency than CSL and RIT.

4.   ROD–SAN: Implementation and Field Trial

In this section, we present our implementation of ROD–SAN and results obtained by field trial which we conducted in order to prove the practicality of ROD–SAN. We only focus on ROD–SAN as its superiority to duty–cycling modes have been confirmed in the previous section. Note that some detailed operations and parameters of ROD–SAN are different from those implemented in the previous section for computer simulations, however, we believe that the implementations of main functionalities and its successful operations in a real–world environment presented in this section are sufficient to show the practical potential of ROD–SAN.

4.1   System Architecture and Protocol Stacks

The implemented system architecture and protocol stacks of ROD–SAN are shown in Fig. 12. The implemented ROD–SAN consists of (1) ROD–SAN nodes that are equipped with sensor and/or actuator, (2) Concentrator that manages ROD–SAN nodes as a sink node and is in charge of protocol conversion, (3) Server (possibly inside the cloud) that collects/sends data/commands from/to ROD–SAN nodes. As mentioned in Sect. 2, the lowest Physical layer (PHY) of each ROD–SAN node is based on IEEE 802.15.4g with 802.15.4 MAC protocol. Among ROD–SAN nodes, RPL [16] is employed in networking layer with 6LoW-PAN [18] to compress IPv6 headers. The application data is transferred among nodes and concentrator with CoAP [19]. The application program is run at each node to read data from sensors, to control actuators, and to manage periodical events triggered with internal timers.

When a node broadcasts a control message toward the surrounding nodes, it needs to wake–up all nodes within the communication range. To this end, we prepare broadcast
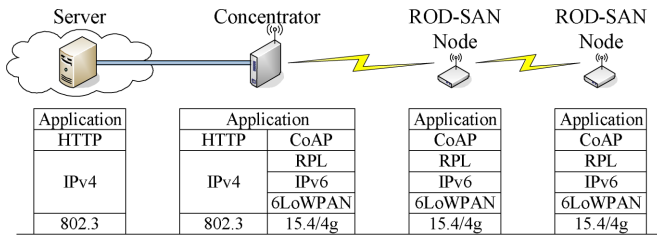
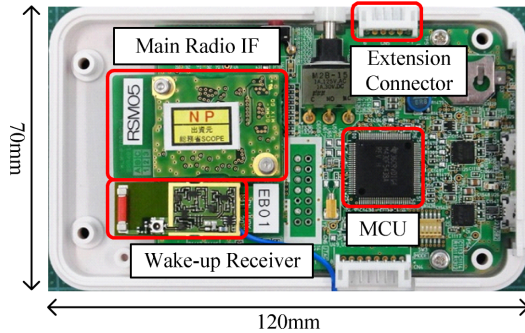**Fig. 12** The system architecture and protocol stacks of ROD–SAN.

Fig. 13 The appearance of a prototype of ROD–SAN node.

Fig. 14 The node deployment in our field trial.

wake–up ID besides unicast wake–up ID. A unique frame length is mapped to broadcast wake–up ID and any wake–up receiver detecting this frame length wakes its main radio IF up. On the other hand, frame length corresponding to unicast ID is in function of MAC address of each node. The function is shared by all nodes, and each node is able to generate an appropriate wake–up signal based on MAC address of the destination node.

4.2 Node Implementation

We developed a prototype of ROD–SAN node whose appearance is shown in Fig. 13. Through the extension connector, we can install any type of sensors and actuators into the node. The main radio IF is based on PHY/MAC protocols of IEEE 802.15.4g/802.15.4 and the wake–up receiver has the configuration shown in Fig. 2. The MCU controls all internal hardware and also executes applications and protocol software presented in Sect. 4.1.

4.3 Experimental Settings

We deployed a single concentrator and 19 nodes over an outdoor area with the scale of $450\,\text{m} \times 200\,\text{m}$ as shown in Fig. 14 where the concentrator is labelled with no. of 0, and nodes, from 1 to 19. The distance among the concentrator and nodes ranges approximately from 50 m to 200 m. The height of node position is set to be 2 m. Inside the measurement area, there is a three–story building with its position and shape shown in Fig. 14. Each node is equipped with a temperature sensor, and programmed to transmit its data every 5 minutes toward the concentrator. Besides sensing operations, we also implemented and evaluated actuation op-
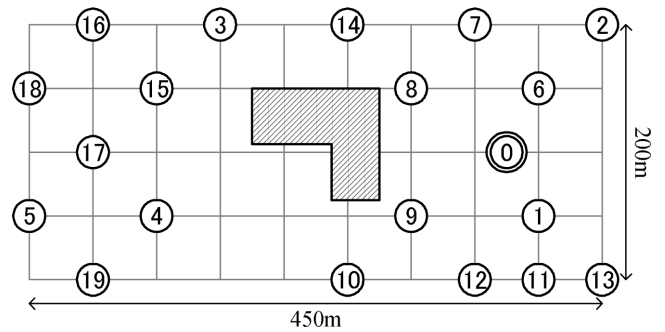
erations in our field trial. Nodes from no. 1 to no. 5 are assumed to have the role of actuator. Each actuator node has LED light on its circuit board, and we consider *actuation* as an action to change the color of LED light. The command of actuation is transmitted from the concentrator at arbitrary timing during the measurement. Note that the concentrator is directly connected to the server through which an operator monitors the collected sensing data and executes the actuation command.

The field trial starts with node deployment, followed by the construction of a tree topology where the concentrator (sink) takes the position of a root by using RPL protocols. Then, the measurement starts when we send a command toward all nodes to start reporting their sensing data to the concentrator. The measurement lasts for 1 hour during which we also send 10 actuation commands to each actuator (i.e., node 1 to node 5). The measurement is conducted for ROD–SAN as well as active WSAN where each node is always active (similar to IEEE 802.15.4 considered in Sect. 3). As for performance metrics, besides the data collection rate, we obtained response time that is used for evaluating the response capability of WSANs. A node with actuator is designed to return a response to the concentrator once it receives an actuation command successfully. When the concentrator does not receive any response from the actuator for 3 seconds, it retransmits the actuation command. The maximum number of retransmissions is set to be 3. We measured the delay from sending an actuation command to the reception of response at the concentrator, and define it as response time. Furthermore, as a metric to evaluate energy–efficiency, we calculated active rate that is defined as the ratio of the period of time during which a node stays in active state to the length of the measurement period. The time of state transition is recorded at each node during the measurement phase, which is used for calculating the active rate. The active rate was used instead of actual energy consumption since it was difficult to measure the accurate circuit current during the measurement.

As radio parameters of IEEE 802.15.4g, we select gaussian frequency shift keying (GFSK) modulation with its transmission power of 20 mW and PHY data rate of 100 kbps. The MAC parameters of IEEE 802.15.4 are set as follows: the minimum back–off exponent (BE) is 3, the

Table 2 Numerical results of field trial.

	Active WSAN	ROD–SAN
Data Collection Rate	98.2%	94.3%
Response Time	1.6 s	2.6 s
Active Rate	100%	9.7%

Fig. 15 An example of tree topology constructed during field trial for ROD–SAN.

maximum BE is 5, and the maximum number of back–off trials is 4. The maximum number of retransmissions for unicast data is set to be 3 with ACK waiting timeout of 4864 μs.

As for wake–up ID of ROD–SAN, we selected 32 frame length to represent each wake–up ID, which are sufficient to differentiate the concentrator and nodes. The minimum length of wake–up frame (ID 0) is 11.56 ms, and we prepare 31 other length with the step of 320 μs. The wake–up ID 0 has a role of broadcast wake–up ID. Since the introduction of wake–up ACK in MAC operations of ROD–SAN makes the implementation with the off–the–shelf 802.15.4g/802.15.4 radio IF complicated, the wake–up ACK is not transmitted after the successful wake–up of each node. This makes it impossible for each node to know the exact timing to start its data transmission. Therefore, after sending a wake–up frame, each node waits for 130 ms before proceeding with the data transmission in order to make sure that the destination is ready to receive the data after successful detection of wake–up signal.

4.4 Experimental Results and Discussions

Table 2 shows experimental results on data collection rate, response time, and active rate (averaged over all nodes) for active WSAN (i.e., WSAN where node is always active) and ROD–SAN, which are all obtained by our field trial. As already pointed out in the previous section, data collection rate and response time of the active WSAN are respectively considered as upper–bound and lower–bound of ROD–SAN. From the results, we can see that ROD–SAN reduces the active rate to the value less than 10% with a little difference of data collection rate and response time as compared with the active WSAN. This means that ROD–SAN has a potential to significantly reduce energy consumption of each node without degrading its reliability and latency. Below, we discuss these results in more detail.

4.4.1 Routing Topology

Figure 15 shows a topology of ROD–SAN, which was constructed during the field trial. From this figure, we can see that ROD–SAN nodes cover the area of 450 m × 200 m with 3–hop from the concentrator at maximum (e.g., node 3 and node 15 in Fig. 15). We also confirmed that the same topology was constructed for active WSAN. This means that each ROD–SAN node has a comparable wake–up range (range within which the wake–up frame is correctly detected) with the communication range of IEEE 802.15.4g.
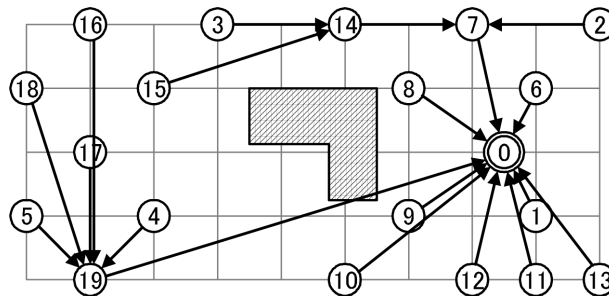
4.4.2 Data Collection Rate

Figure 16 shows data collection rate against number of hops that are required for each node to transmit data toward the concentrator. From this figure, we can see that data collection rate is degraded as the required number of hops is increased. The failure of data delivery at each link can be caused by interference and frame collisions among different nodes. Each node attempts to transmit control messages at arbitrary timing, such as messages for RPL and Neighbor Unreachability Detection message for Neighbor Discovery Protocol of IPv6, besides the periodical transmissions of sensing data. Due to the interference caused by these transmissions, timeout can occur during carrier–sensing (i.e. the maximum number of back–offs is reached before transmitting data) and some nodes suffer from hidden terminal problem that increases the probability of frame collisions. As the number of hops is increased, each data needs to pass through more links exposed to these problems, which degrades the data collection rate for higher number of hops.

The degradation of data collection rate of ROD–SAN as compared with active WSAN is mainly caused by two reasons. First, ROD–SAN requires each node to transmit a wake–up frame every time it transmits data or control message. This increases the total number of frames to be transmitted by each node, which results in a larger amount of interference observed over the channel. Second, due to the absence of wake–up ACK, data frame is transmitted even if the wake–up frame is not correctly detected at the corresponding destination. The wake–up failures can be caused by the interference/collision with the other frames as well as small and/or fluctuated received signal levels of wake-up frames due to attenuation and/or fading. The reliability can be increased by introducing the wake–up ACK into our implementations. However, even with the introduction of wake–up ACK and retransmissions of wake–up frame, the wake–up failures can increase the data delivery latency at each hop. Furthermore, retransmissions can cause each sender node to spend more energy, which negatively affects the overall energy–efficiency of ROD–SAN. The solutions to these problems related to wake-up failures will be developed in our future work.
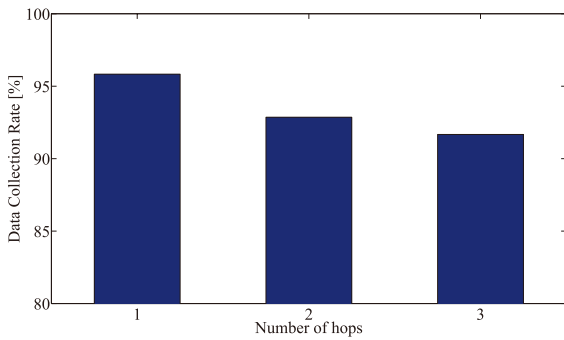
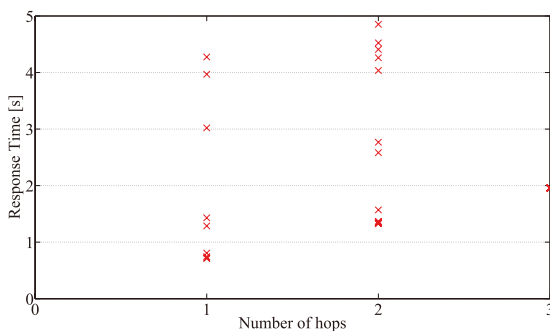**Fig. 16**   Data collection rate against number of hops for ROD–SAN.

Fig. 18   Active rate against node no. for ROD–SAN.

Fig. 17   Response time against number of hops for ROD–SAN.

4.4.3   Response Time

Figure 17 shows the distribution of response time for each number of hops between the concentrator and nodes. Here, we first notice that the minimum response time for each number of hops linearly increases by around 600 ms as the number of hops increases. With ROD–SAN, the wake–up delay (the total duration of transmission of wake–up frame and wake–up process of each node) is around 300 ms. This delay precedes transmissions of actuation command and its response, therefore, with the increase of 1–hop, a fixed amount of additional delay of around 600 ms is observed for the minimum response time. Furthermore, we can see that the response time can largely deviate from its minimum value. This is due to the transmission failures of actuation command and its response, which are caused by the interference and frame collisions as explained in discussions on data collection rate.

4.4.4   Active Rate

The active rate of each ROD–SAN node is shown in Fig. 18. The active rate of each node largely depends on its positioning within the constructed tree topology and link quality against its parent node. When a node accommodates many child nodes, it is woken up frequently for forwarding their data. Furthermore, when the quality of forwarding link against the parent node is worse, the number of retrans-
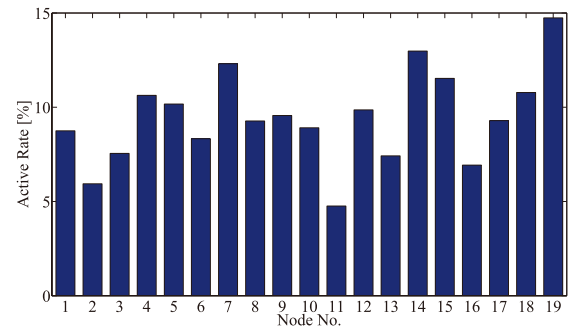
missions is increased, which requires a node to be in active state for longer period. This relationship is clearly seen in Fig. 15 and Fig. 18. For instance, node 19 has many child nodes with a long–distance forwarding link to the concentrator as shown in Fig. 15, resulting in the largest active rate in Fig. 18.

From all the above experimental results, we can conclude that ROD–SAN has a practical potential to significantly reduce energy consumption of each WSAN node while keeping high reliability and low latency.

5.   Conclusions

In this paper, we have focused on ROD–SAN, a WSAN where the wake–up receiver and on–demand data transmissions are employed for realizing high–response and energy–efficient WSAN. We have first shown that ROD–SAN can improve reliability, latency, and energy–efficiency of WSANs in comparison to standard duty–cycling modes defined in IEEE 802.15.4e. Then, we have presented implementations including overall protocol stacks required for ROD–SAN, i.e., from wake–up signaling at node/PHY level to the application layer offering the functionalities of information monitoring and networked control. We have shown experimental results obtained through our field trial in which 20 nodes are deployed in an outdoor area with the scale of 450 m × 200 m. The numerical results have shown that we can reduce active rate of each node to the value less than 10% while keeping the small deviation of data collection rate and response time from their upper and lower bounds. With these results, we have validated a practical potential for ROD–SAN to significantly reduce energy consumption of each node without degrading its reliability and latency.

Our field trial revealed not only the potential of ROD–SAN but also some limitations and problems as discussed during the text, e.g., the absence of wake–up ACK to confirm the successful wake–up. In our future work, we will include it with some cross–layer designs considering interactions between wake–up mechanisms and protocols in higher layers. We are also planning to extend our prototype and field trial so that we can conduct experiments for diverse types of WSANs with different topologies.

Acknowledgement

References

[1] I.F. Akyildiz and I.H. Kasimoglu, "Wireless sensor and actor networks: research challenges," Ad Hoc Networks, vol.2, no.4, pp.351–367, Oct. 2004.

[2] H. Ramamurthy, B.S. Prabhu, R. Gadh, and A.M. Madni, "Wireless industrial monitoring and control using a smart sensor platform," IEEE Sensors J., vol.7, no.5, pp.611–618, May 2007.

[3] Y. Zhang, A. Breeschoten, X. Huang, N. Kiyani, A. Ba, P. Harpe, K. Imamura, R. de Francisco, V. Pop, G. Dolmans, and H. de Groot, "Improving energy-efficiency in building automation with event-driven radio," Proc. 2011 International Conference on Wireless Communications and Signal Processing (WCSP), pp.1–5, 2011.

[4] N. Bressan, L. Bazzaco, N. Bui, P. Casari, L. Vangelista, and M. Zorzi, "The deployment of a smart monitoring system using wireless sensor and actuator networks," Proc. 2010 First IEEE International Conference on Smart Grid Communications, pp.49–54, 2010.

[5] R.C. Carrano, D. Passos, L.C.S. Magalhaes, and C.V.N. Albuquerque, "Survey and taxonomy of duty cycling mechanisms in wireless sensor networks," IEEE Commun. Surv. Tutorials, vol.16, no.1, pp.181–194, Feb. 2014.

[6] IEEE-SA Standards Board, "802.15.4e-2012 — IEEE standard for local and metropolitan area networks–Part 15.4: Low-rate wireless personal area networks (LR-WPANs) Amendment 1: MAC sublayer," IEEE Standard, 2012.

[7] I. Demirkol, C. Ersoy, and E. Onur, "Wake-up receivers for wireless sensor networks: Benefits and challenges," IEEE Wireless Commun., vol.16, no.4, pp.88–96, Aug. 2009.

[8] K. Abe, A. Hasegawa, S. Sakata, T. Ikenaga, and H. Yomo, "Proposal and evaluation of radio-on-demand sensor and actualtor networks," IEICE Technical Report, NS2013-221, 2014.

[9] T. Ikenaga, H. Yomo, A. Hasegawa, K. Abe, D. Nobayashi, and T. Ito, "Radio-on-denamd networks for green wireless access," IEICE Trans. Commun. (Japanese Edition), vol.J99-B, no.4, pp.261–274, April 2016.

[10] "Low-rate wireless personal area networks (LR-WPANs), Amendment 3: Physical layer (PHY) specification for low-data-rate, wireless, smart metering utility networks, IEEE Std.802.15.4g, 2012."

[11] V. Jelicic, M. Magno, D. Brunelli, V. Bilas, and L. Benini, "Analytic comparison of wake-up receivers for WSNs and benefits over the wake-on radio scheme," Proc. 7th ACM Workshop on Performance Monitoring and Measurement of Heterogeneous Wireless and Wired Networks, PM2HW2N'12, pp.99–106, 2012.

[12] K. Chebrolu and A. Dhekne, "Esense: Energy sensing-based cross-technology communication," IEEE Trans. Mobile Comput., vol.12, no.11, pp.2303–2316, Nov. 2013.

[13] M. Patel and D. Wang, "Energy efficient methods of encoding destination address to address overhearing problem in BAN," Proc. 2010 IEEE 21st International Symposium on Personal, Indoor and Mobile Radio Communications Workshops, pp.101–106, 2010.

[14] Y. Kondo, H. Yomo, S. Tang, M. Iwai, T. Tanaka, H. Tsutsui, and S. Obana, "Energy-efficient WLAN with on-demand AP wake-up using IEEE 802.11 frame length modulation," Comput. Commun., vol.35, no.14, pp.1725–1735, Aug. 2012.

[15] IEEE-SA Standards Board, "IEEE Standard for Local and metropolitan area networks — Part 15.4: Low-rate wireless personal area networks," IEEE Standard, 2011.

[16] T. Winter, Ed., P. Thubert, Ed., A. Brandt, J. Hui, R. Kelsey, P. Levis, K. Pister, R. Struik, J.P. Vasseur, and R. Alexander, "RPL: IPv6 routing protocol for low power and lossy networks," IETF, RFC 6550, March 2012.

[17] R. Jurdak, A.G. Ruzzelli, and G.M.P. O'Hare, "Radio sleep mode optimization in wireless sensor networks," IEEE Trans. Mobile Comput., vol.9, no.7, pp.955–968, July 2010.

[18] "6LoWPANs: IPv6 over low-power wireless personal area networks," IETF RFC 4944/6282/6775, Nov. 2012.

[19] Z. Shelby, K. Hartke, and C. Bormann, "The constrained application protocol (CoAP)," IETF, RFC 7252, June 2014.

Hiroyuki Yomo received B.S., M.S., and Ph.D. degrees in communication engineering from Osaka University, Japan, in 1997, 1999 and 2002, respectively. From April 2002 to March 2004, he was a Post-doctoral Fellow at Aalborg University, Denmark. From April 2004 to September 2004, he was at NEC Corporation, Japan. In October 2004, he joined Aalborg University, Denmark, as an Assistant Research Professor, and worked as an Associate Professor from February 2006 to March 2008. From April 2008 to March 2010, he was a senior researcher at ATR, Japan. In April 2010, he joined Kansai University, Japan, as an Associate Professor, and has been a Professor since April 2015. He is also affiliated with ATR as a guest researcher. He received the 2010 Funai Academic Award from Funai Foundation for Information Technology. He has received several best paper awards, including the one at IEEE Globecom 2009. His main research interests are access technologies, radio resource management, and link-layer techniques in the broad area of wireless communications.

Takahiro Kawamoto received B.S., and M.S. degrees in Electrical and Electronic engineering from Kansai University, Japan, in 2014 and 2016, respectively. His research interests include PHY/MAC protocol designs for wireless sensor networks.

Kenichi Abe received B.S. degrees in Electronic engineering from The Tohoku institute of Technology, in 1997. From 1997 to 2003, he worked in NEC Miyagi, Ltd. Since 2003, he has been with NEC Communication Systems, Ltd., and is currently an expert at Advanced Technology Development Group where he is engaged in research and development of wireless networks.

Yuichiro Ezure received B.S. degrees in Applied Physics from The Tokyo University of Science, in 2001. From 2001 he has been with NEC Communication Systems, Ltd., and is currently an assistant manager at Advanced Technology Development Group where he is engaged in research and development of wireless networks.

Tetsuya Ito received B.S., and M.S. degrees in Electronic engineering from The University of Electro-Communications, in 1994 and 1996, respectively. From 1996 to 2002, he worked in NEC Telecom Systems, Ltd. Since 2003, he has been with NEC Communication Systems, Ltd., and is currently a senior manager at Advanced Technology Development Group where he is engaged in research and development of wireless networks. He is a member of IEEE.

Akio Hasegawa received B.E., M.E., and D.E. degrees in electrical engineering from Meiji University in 1995, 1997, and 2000, respectively. He was a research assistant in Electrical Engineering Department of Gifu University before joining Communication Research Laboratories (CRL), now the National Institute for Information and Communication Technology (NICT) as a research associate in 2002. In 2004 he joined ATR Adaptive Communications Research Laboratories as a researcher. Since 2013, he has been the Head of the Department of Smart Networks of ATR. His research interests include ad-hoc networks, cognitive radio systems. He is a member of the IEEE.

Takeshi Ikenaga received B.E., M.E., and D.E. degrees in computer science from Kyushu Institute of Technology, Iizuka, Japan in 1992, 1994, and 2003, respectively. From 1994 to 1996, he worked at NEC Corporation. From 1996 to 1999, he was an assistant professor in the Information Science Center, Nagasaki University. From 1999 to 2004, he was an assistant professor in the Department of Computer Science and Electronics, Faculty of Computer Science and Systems Engineering, Kyushu Institute of Technology. From March 2004 to 2011, he was an associate professor in the Department of Electrical, Electronic and Computer Engineering, Faculty of Engineering, Kyushu Institute of Technology. Since 2011, he has been a professor in the Department of Electrical, Electronic and Computer Engineering, Faculty of Engineering, Kyushu Institute of Technology. His research interests include performance evaluation of computer networks, wireless LANs and QoS routing. He is a member of the IEEE and IEICE.